Supplementary Information (SI) for Journal of Materials Chemistry C.

Variation in the Zero-Point Energy Difference via Electrostatic Interactions in Co(II)-Cltpy-based Spin-crossover Molecular Materials

Mousumi Dutta[1], Ajana Dutta[2#], Prabir Ghosh[3,5#]*, Shubhankar Maiti[1#], Laurentiu Stoleriu[4], Cristian Enachescu[4], Pradip Chakraborty[1]*

[1]Department of Chemistry, Indian Institute of Technology Kharagpur, Kharagpur-721302, India

[2]Department of Physics, Indian Institute of Technology Kharagpur, Kharagpur-721302, India

[3]Department of Mechanical Engineering, Indian Institute of Technology Kharagpur, Kharagpur-721302, India

[4]Faculty of Physics, Al. I. Cuza University, 700506 Iasi, Romania

[5]Current address: Centre for Interdisciplinary Science, JIS Institute of Advanced Studies and Research (JISIASR) Kolkata, JIS University, GP Block, Sector-5, Salt Lake, Kolkata-700091, West Bengal, India

# Contributed equally to this work

*Corresponding Author, E-mail: pradipc@chem.iitkgp.ac.in; prabir.chem@gmail.com

FTIR:

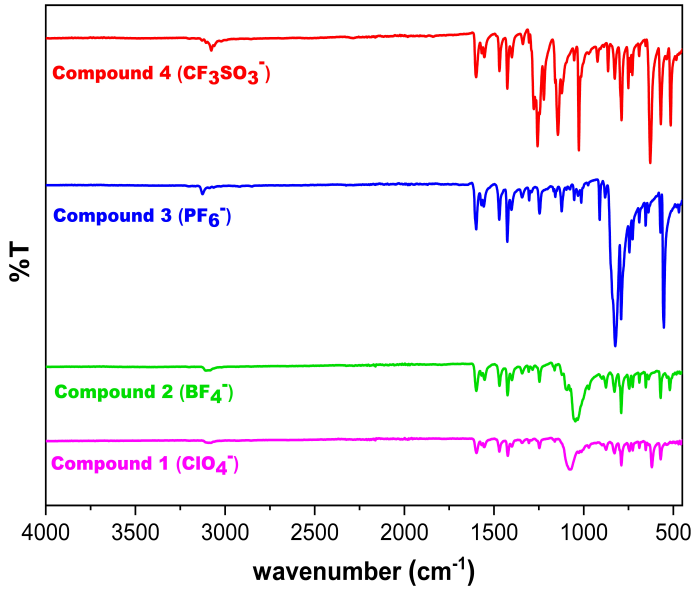

Figure S1: FTIR spectra of the as-synthesized compounds 1-4

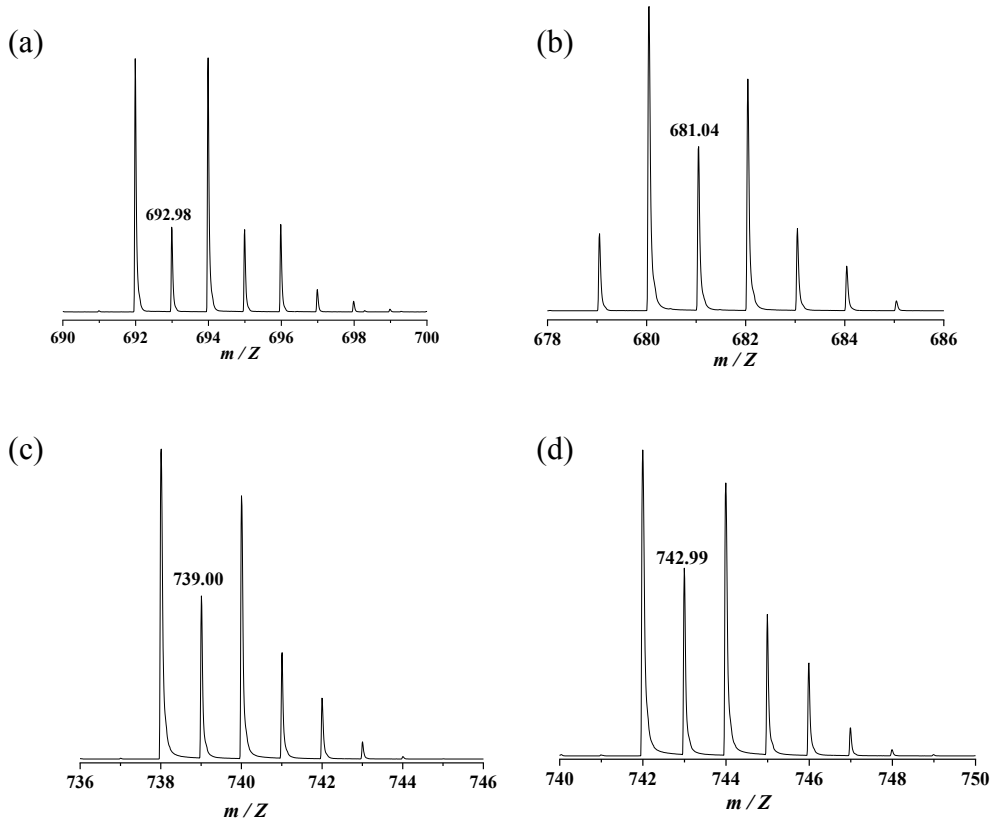

Figure S2. Experimental HRMS (+ve mode) spectra of (a){1-ClO_4}$^+$, (b) {2-BF_4}$^+$, (c) {3-PF_6}$^+$ and (d) {4-CF_3SO_3}$^+$ in CH_3CN.

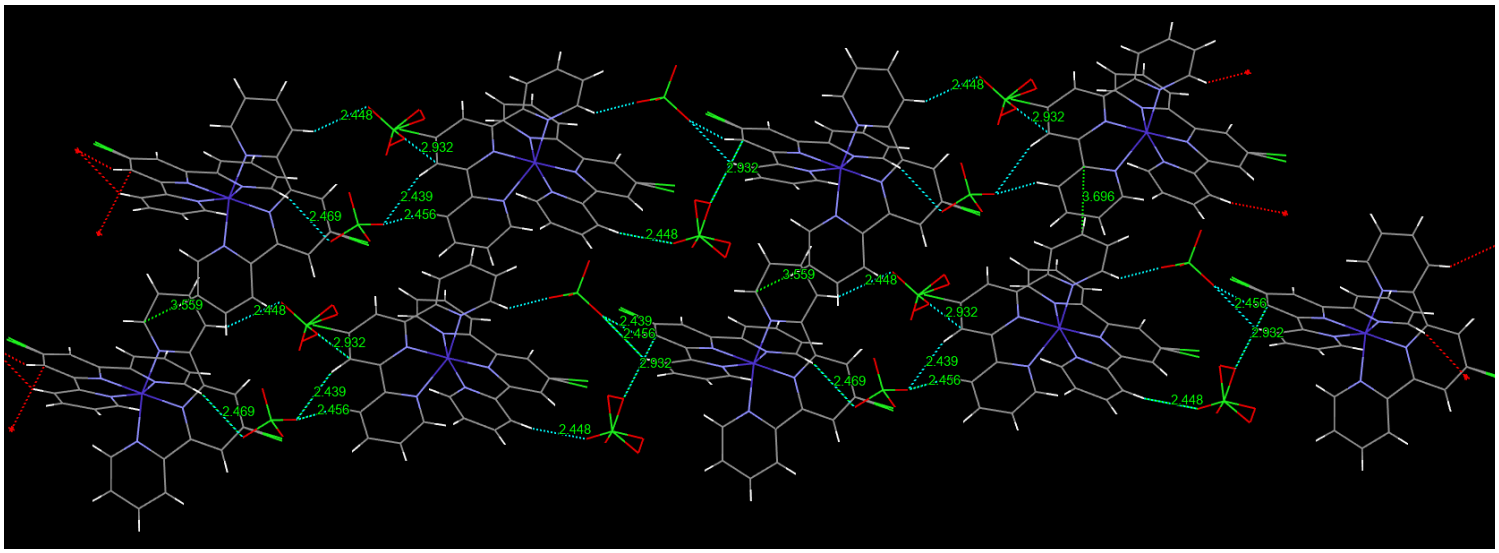

Figure S3: 1D chain-like stacked crystal packing pattern for compound 1 (i.e., ClO_4^-) upon growing the unit cell showing both intra-chain and inter-chain interactions (comparatively strong) with the relevant interaction lengths providing the strong effective crystal field strength around the Co(II)-spin-crossover centers.

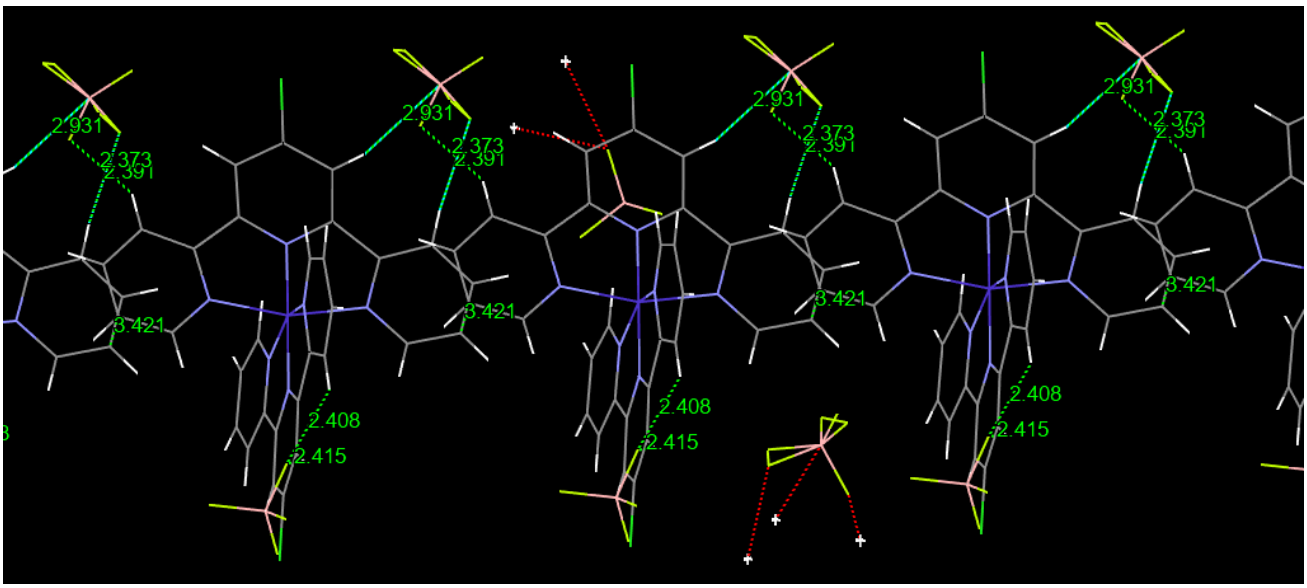

Figure S4: 1D chain-like crystal packing pattern for compound 2 (i.e., BF_4^-) upon growing the unit cell showing only intra-chain interactions (comparatively weak) with the relevant interaction lengths providing the moderately weak effective crystal field strength around the Co(II)-spin-crossover centers.

.

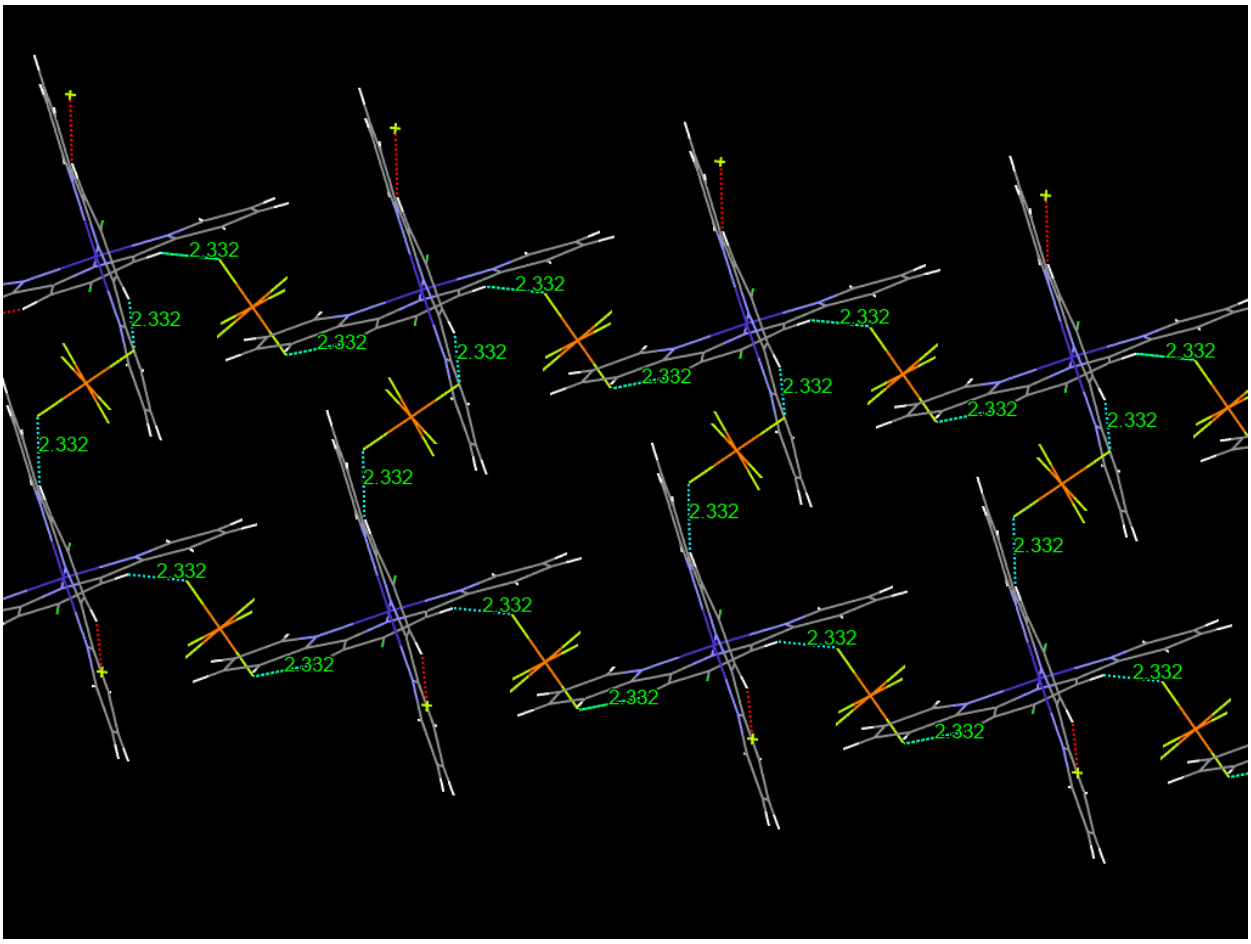

Figure S5: 1D chain-like stacked crystal packing pattern for compound 3 (i.e., PF_6^-) upon growing the unit cell showing both intra-chain and inter-chain interactions (comparatively strong) with the relevant interaction lengths providing the strong effective crystal field strength around the Co(II)-spin-crossover centers.

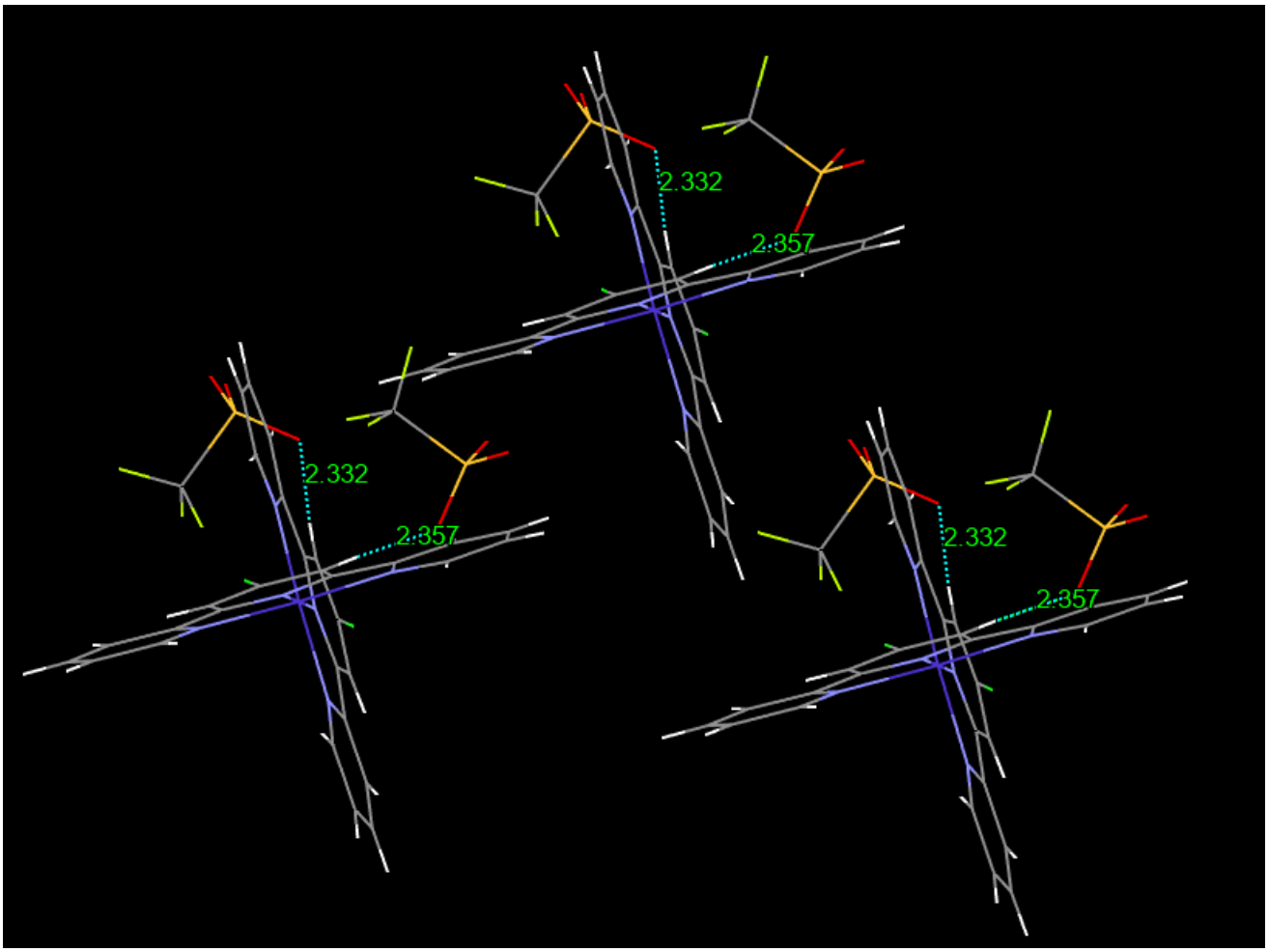

Figure S6: Crystal packing pattern for compound 4 (i.e., $CF_3SO_3^-$) shows discrete individual molecular moieties without any intra- and inter-chain molecular interactions providing the weakest effective crystal field strength around the Co(II)-spin-crossover centers.

Powder X-ray diffraction (PXRD):

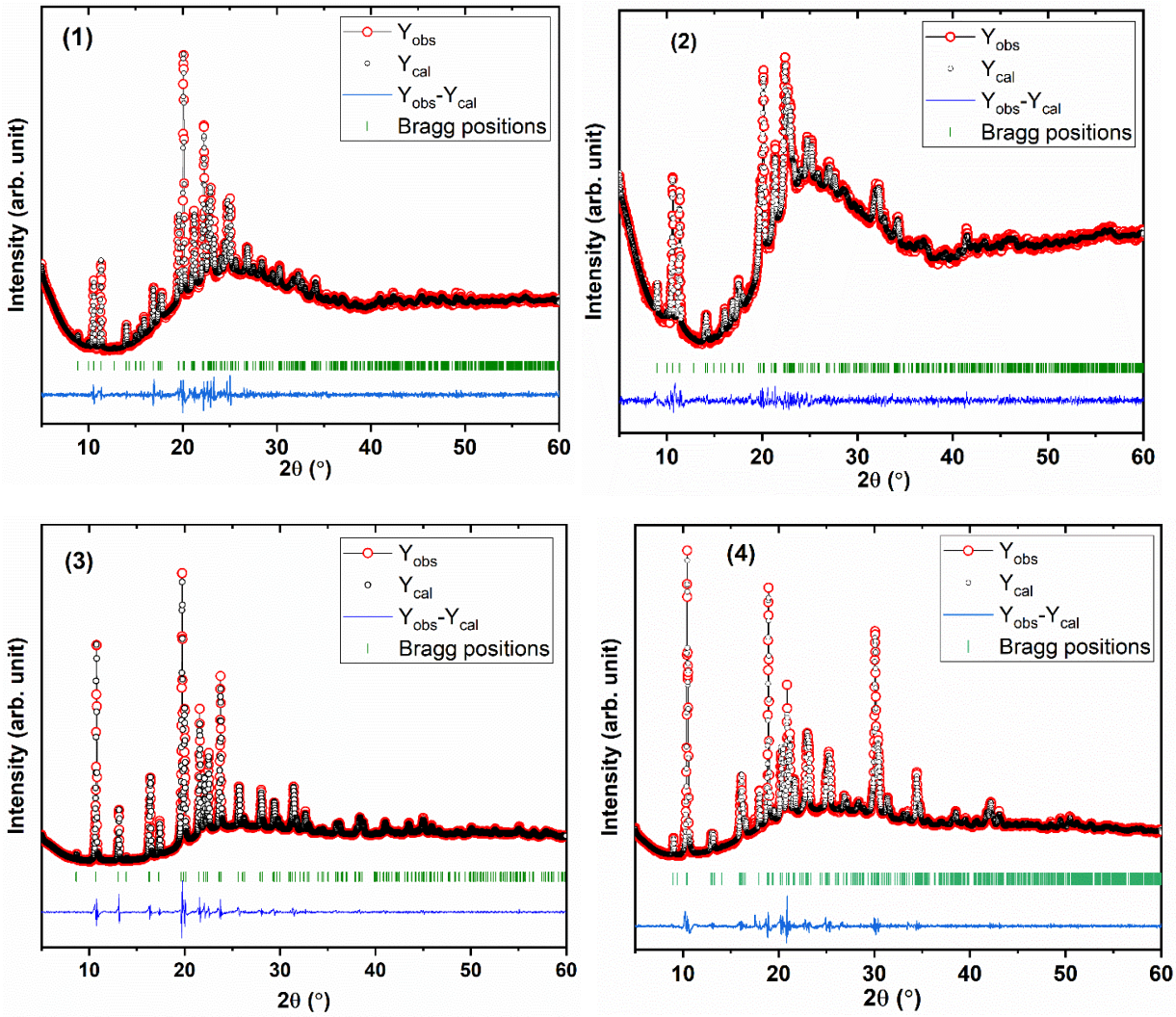

Figure S7: PXRD Le Bail profile refinement of $[Co(terpy\text{-}Cl)_2](ClO_4)_2$, (1, top left); $[Co(terpy\text{-}Cl)_2](BF_4)_2$, (2, top right); $[Co(terpy\text{-}Cl)_2](PF_6)_2$, (3, bottom left); and $[Co(terpy\text{-}Cl)_2](CF_3SO_3)_2$, (4, bottom right) at room temperature.

EPR spectroscopy:

Table S1. EPR data of compound 1-4 at 8 K.

Compound	g_z	g_y	g_x	$\langle g \rangle^a$	Δg^b
1	2.303	2.040	1.958	2.078	0.345
2	2.308	2.076	1.957	2.070	0.351
3	2.247	1.997	1.953	2.119	0.294
4	2.226	2.050	1.948	2.105	0.278

$\langle g \rangle^a = ((1/3)(g_z^{\,2} + g_y^{\,2} + g_x^{\,2}))^{1/2}$, $\Delta g^b = g_z - g_x$